

AN HST/COS SEARCH FOR WARM-HOT BARYONS IN THE MRK 421 SIGHTLINE

CHARLES W. DANFORTH, JOHN T. STOCKE, BRIAN A. KEENEY, STEVEN V. PENTON, J. MICHAEL SHULL, YANGSEN YAO & JAMES C. GREEN

CASA, Department of Astrophysical and Planetary Sciences, University of Colorado, 389-UCB, Boulder, CO 80309;
 danforth@colorado.edu

ApJ accepted July 2011

ABSTRACT

Thermally-broadened Ly α absorbers (BLAs) offer an alternate method to using highly-ionized metal absorbers (O VI, O VII, etc.) to probe the warm-hot intergalactic medium (WHIM, $T = 10^5 - 10^7$ K). Until now, WHIM surveys via BLAs have been no less ambiguous than those via far-UV and X-ray metal-ion probes. Detecting these weak, broad features requires background sources with a well-characterized far-UV continuum and data of very high quality. However, a recent HST/COS observation of the $z = 0.03$ blazar Mrk 421 allows us to perform a metal-independent search for WHIM gas with unprecedented precision. The data have high signal-to-noise ($S/N \approx 50$ per ~ 20 km s $^{-1}$ resolution element) and the smooth, power-law blazar spectrum allows a fully-parametric continuum model. We analyze the Mrk 421 sight line for BLA absorbers, particularly for counterparts to the proposed O VII WHIM systems reported by Nicastro et al. (2005a,b) based on *Chandra*/LETG observations. We derive the Ly α profiles predicted by the X-ray observations. The signal-to-noise ratio of the COS data is high ($S/N \approx 25$ per pixel), but much higher S/N can be obtained by binning the data to widths characteristic of the expected BLA profiles. With this technique, we are sensitive to WHIM gas over a large (N_H, T) parameter range in the Mrk 421 sight line. We rule out the claimed Nicastro et al. O VII detections at their nominal temperatures ($T \sim 1 - 2 \times 10^6$ K) and metallicities ($Z = 0.1 Z_\odot$) at $\gtrsim 2\sigma$ level. However, WHIM gas at higher temperatures and/or higher metallicities is consistent with our COS non-detections.

Subject headings: intergalactic medium, quasars: absorption lines, cosmology: observations, BL Lacertae objects: individual (Mrk 421)

1. INTRODUCTION

The Warm-Hot Intergalactic Medium (WHIM) is expected to make up 25–50% of the baryons in the low-redshift Universe based on cosmological simulations (Cen & Ostriker 1999; Davé et al. 1999, 2001; Smith et al. 2011). Thus far, only a small fraction of this hot gas has been detected (see, e.g. Danforth 2009), and the interpretation of these detections is still controversial. The difficulty in detecting this gas lies in its combination of high temperature ($10^5 - 10^7$ K) and low hydrogen density ($10^{-4} - 10^{-6}$ cm $^{-3}$). For example, only the subset of WHIM gas which is sufficiently metal-enriched can be detected through highly-ionized metal ions at UV and X-ray energies. The O VI $\lambda\lambda 1031, 1037$ doublet has been detected in numerous extragalactic systems with the *Far Ultraviolet Spectroscopic Explorer* (FUSE) and *Hubble Space Telescope* (HST) (Danforth & Shull 2005, 2008; Tripp et al. 2008; Thom & Chen 2008). It may trace very low density, photoionized $\sim 10^4$ K gas (e.g., Oppenheimer & Davé 2008; Oppenheimer et al. 2011) or shock-heated, collisionally-ionized WHIM (Smith et al. 2011). Until now, the searches for hotter WHIM ($> 10^6$ K) have been restricted to soft X-ray absorption.

Very highly ionized metal species such as O VII, O VIII, N VII and Ne IX with soft-X-ray resonance transitions offer a good option for finding diffuse gas at the hotter end of the WHIM temperature range. However, the predicted low metallicity of this gas ($Z \sim 0.1 Z_\odot$ typical of O VI absorbers; Danforth & Shull 2008) and the relative insensitivity and low resolution of even our best,

current X-ray spectrometers (i.e., the *Chandra* Low Energy Transmission Grating (LETG) and *XMM-Newton* Reflection Grating Spectrometer (RGS)) has generated controversy for most or all current proposed detections of hotter WHIM gas.

The growing number of “broad Ly α absorbers” (BLAs) detected in high signal-to-noise FUV spectra (Sembach et al. 2004; Richter et al. 2004, 2006; Lehner et al. 2007; Danforth et al. 2010a) may trace WHIM independent of metal enrichment, but this diagnostic suffers from a different set of observational uncertainties. Even at the cooler end of the WHIM temperature range, the fraction of hydrogen in a neutral state is tiny. Thermal broadening renders any Ly α absorption shallow and broad, and the WHIM absorber may be blended with narrower absorption features arising in adjacent, cooler, photoionized gas. At temperatures above 10^6 K, spectra of extremely high quality, with well-defined continua, are required to characterize the WHIM through BLAs alone. Independent measurements of individual WHIM systems through complimentary techniques reduce the uncertainties inherent in single-method detections.

Two of the earliest and most-cited X-ray WHIM detections were the two reported O VII absorbers (Nicastro et al. 2005a,b) in *Chandra* LETG observations of the blazar Mrk 421 ($z_{em} = 0.030$). These observations were made while Mrk 421 was in a flaring state and represent some of the highest signal-to-noise soft-X-ray data taken to date on an extragalactic

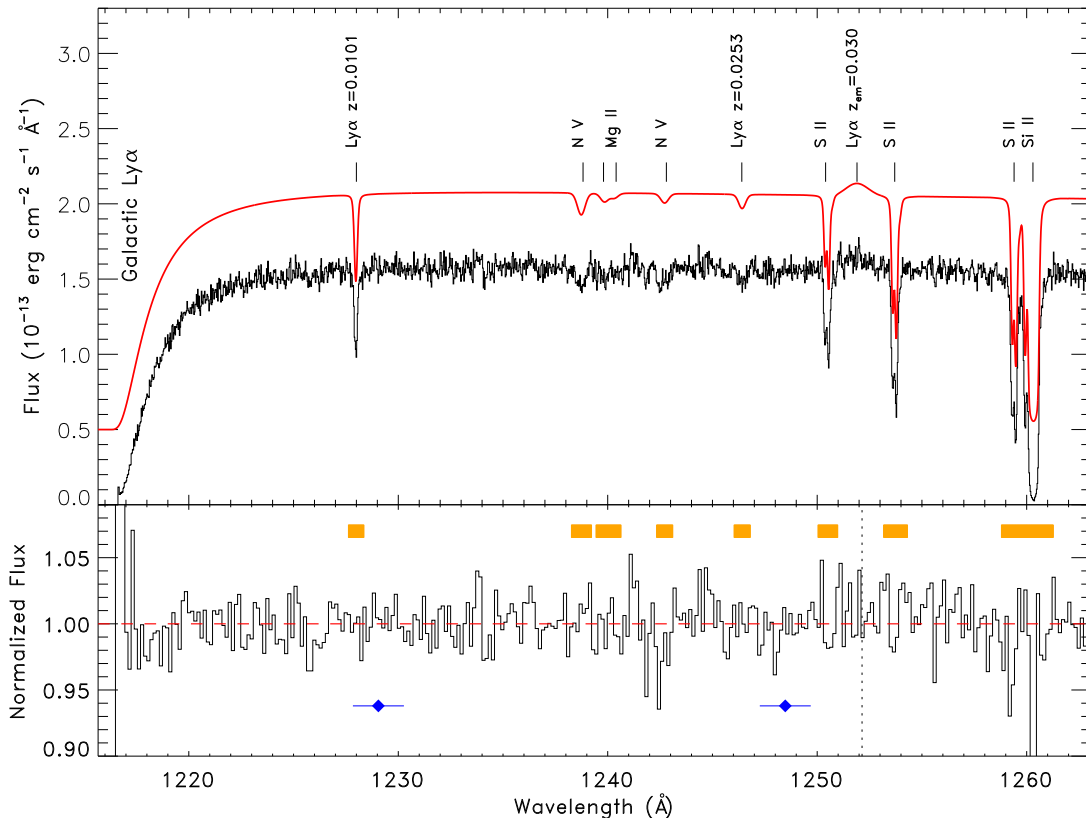


FIG. 1.— HST/COS spectrum of Mrk 421 spanning the entire redshift pathlength of the Ly α forest ($1216\text{\AA} < \lambda < 1252\text{\AA}$). The data in the top panel are binned by three pixels ($\sim 1/2$ resolution element). The power-law continuum, Galactic damped Ly α absorption, intrinsic Ly α emission ($z_{em} = 0.030$), and known narrow absorption features detailed in the text are modeled by the red curve offset from the flux by $+5 \times 10^{-14} \text{ erg cm}^{-2} \text{ s}^{-1} \text{ \AA}^{-1}$. The lower panel shows the residual data binned by seven pixels (approximately the COS resolution element) after the continuum and all absorption/emission features are divided out. The regions where narrow lines have been modeled out of the data are shown by orange bars. Blue diamonds mark the redshift locations and $\pm 300 \text{ km s}^{-1}$ uncertainties of the Nicastro et al. (2005a) claimed O VII features.

sight line. Although these absorbers were *not confirmed* in observations by *XMM-Newton* (Kaastra et al. 2006; Williams et al. 2006; Rasmussen et al. 2007), their presence has neither been confirmed nor ruled out conclusively. While a few other X-ray WHIM absorption detections have been proposed (e.g., in the PKS 2155-304 sight line by Fang et al. 2002), a new tactic employed by Buote et al. (2009) may have finally achieved some success. Based on the results of simulations (e.g., Davé et al. 1999) that show high concentrations of WHIM gas around large-scale filamentary structure, Buote et al. (2009) (see also Fang et al. 2010; Zappacosta et al. 2010) observed the bright blazar H 2356–309 behind the Sculptor Wall and made O VII detections at the redshift of that filament with both *Chandra* and *XMM-Newton*. Based on the Sculptor Wall detection, it seems worthwhile to revisit the Mrk 421 sight line, since one of the two claimed WHIM detections is at the redshift ($z = 0.027$) of another nearby, large-scale galaxy filament, the Great Wall (de Lapparent, Geller & Huchra 1986; Penton, Stocke, & Shull 2000; Williams et al. 2010).

In this paper, we focus on the potential for detecting WHIM in high-quality UV spectra from the Cosmic Origins Spectrograph (COS) on HST. This analysis is specific to the Mrk 421 sight line, but easily generalized to

sight lines for which high-quality far-UV spectra exist. The FUV spectra of blazars can be well-modeled as a power law (Stocke, Danforth, & Perlman 2011), and the high S/N and multiple ionic transitions allow foreground Galactic absorbers to be well-modeled. Since the data can be fitted with a fully parametric continuum model, this is an ideal test-bed for detecting WHIM gas in BLAs.

In Section 2, we present the COS FUV spectrum of Mrk 421, identify all spectral features present, both Galactic and extragalactic, and produce a normalized, line-free spectrum covering the entire Ly α forest region. In Section 3, we model the BLA absorbers implied by both the reported Nicastro et al. (2005a,b) (henceforth collectively N05) O VII measurements and for more generalized WHIM absorbers. We then place limits on the temperature and metallicity of any WHIM gas present along the Mrk 421 line of sight based on the observed COS data. In Section 4 we discuss the meaning and importance of these results, reiterate our main conclusions, and discuss applications to other sight-lines.

2. OBSERVATIONS AND ANALYSIS

COS far-UV observations of BL Lac object Mrk 421 ($z_{em} = 0.030$) were carried out in 2009, December, during the first three months of COS science obser-

uations as part of the COS Guaranteed Time Observations (PID 11520, PI Green). Four exposures were made in the G130M ($1135 \text{ \AA} < \lambda < 1480 \text{ \AA}$; totalling 1.7 ksec) medium-resolution grating ($R \approx 18,000$), each at a different central wavelength setting, to dither over known instrumental features (see Green et al. 2011; Osterman et al. 2011).

The exposures were reduced with a custom flat field derived from the combination of several public COS calibration observations of white dwarfs. Four targets were used to create the G130M flat field; WD 0308–565, WD 0320–539, WD 0947+857, and WD 1057+719. For each calibration target, an iterative technique was used to independently measure the relatively smooth continua from the inferred underlying flat-field and grid wire shadows using the ‘x1d’ files output by CALCOS 2.13. The four independent one-dimensional estimates of the G130M flat field were merged in detector space with $(S/N)^2$ weighting. After applying the custom flat field to each exposure, we aligned the four Mrk 421 exposures in wavelength space via a cross-correlation of regions around prominent ISM absorption features. Exposures were interpolated onto a common wavelength grid and combined via an exposure time weighted mean as described in Danforth et al. (2010b).

Our custom flat field is not perfect, but it consistently improved the continuum signal-to-noise in our Mrk 421 spectrum as compared to the standard “wireflat” processing (Danforth et al. 2010b). For example, in the 1410–1430 \AA region of the Mrk 421 G130M spectrum, where no ISM or IGM absorption lines are expected, the signal-to-noise per seven-pixel resolution element improved from 27 to 36 with our custom flat fielding, as compared to our standard “wireflat” processing. A second line-free region from 1340–1369 \AA increased from S/N of 38 to 48 per resolution element.

2.1. Spectral Modeling

The Ly α forest region of the Mrk 421 sight-line is shown in the top panel of Figure 1. Since we are interested in weak, broad absorption features in the data, an accurate and detailed model fit to the spectrum including all known features is crucial. Fortunately, as with most blazars, the dereddened UV continuum is easily defined by a power law of the form $F_\lambda = F_{912} (\lambda/912 \text{ \AA})^{-\alpha_\lambda}$. We use the parameters $F_0 = 3.405 \times 10^{-13} \text{ erg cm}^{-2} \text{ s}^{-1} \text{ \AA}^{-1}$ and $\alpha_\lambda = 1.918 \pm 0.020$ to provide a baseline continuum fit to the data in the 1150 \AA –1300 \AA region. Note that these parameters are slightly different from those reported by Stocke, Danforth, & Perlman (2011), which were based on an earlier reduction of the data and a continuum fit to the entire COS/FUV spectral region. The damped Galactic Ly α absorber is modeled with the parameters $v = -28 \pm 1 \text{ km s}^{-1}$, $b_{\text{HI}} = 55 \pm 2 \text{ km s}^{-1}$, and $\log N_{\text{HI}} (\text{cm}^{-2}) = 20.042 \pm 0.002$. This is consistent with the emission-weighted mean H I 21 cm profile in a $\sim 0.6^\circ$ beam toward Mrk 421 in the Leiden-Argentine-Bonn H I survey (LAB, Kalberla et al. 2005). The measured column of neutral hydrogen corresponds to a Galactic reddening of $E(B - V) = N_{\text{HI}}/5.8 \times 10^{21} \text{ cm}^{-2} = 0.019$. (A fit to the Galactic Ly β profile in the *FUSE* data yields a consistent value.) In a departure from the pure power-law source continuum typical of BL Lac objects,

Mrk 421 shows a weak emission feature at 1251.9 \AA corresponding to Ly α emission at $z_{\text{em}} = 0.0298$ from circumnuclear gas in the blazar. We include the fit from Stocke, Danforth, & Perlman (2011) ($FWHM = 1.23 \text{ \AA}$, $I = 1.27 \times 10^{-14} \text{ erg cm}^{-2} \text{ s}^{-1}$) in our spectral model, shown offset from the data in the top panel of Figure 1.

There are several narrow Galactic absorption lines which can be modeled out of the spectrum. The stronger blue line of the N V $\lambda\lambda 1238.82, 1242.80$ doublet is well fitted with parameters $v = -21 \pm 6 \text{ km s}^{-1}$, $b = 59 \pm 8 \text{ km s}^{-1}$, and $\log N_{\text{NV}} = 13.34 \pm 0.05$, but the weaker red line of the doublet shows an absorption excess that is discussed below. The S II 1259.52, 1253.81, 1250.58 \AA triplet has a strong Galactic component ($v = -8 \pm 2 \text{ km s}^{-1}$, $b = 13 \pm 4 \text{ km s}^{-1}$, $\log N_{\text{SII}} = 15.05 \pm 0.10$), a weaker, blue-shifted component ($v = -48 \pm 2 \text{ km s}^{-1}$, $b = 14 \pm 5 \text{ km s}^{-1}$, $\log N_{\text{SII}} = 14.89 \pm 0.05$), and very weak red wing ($v = 32 \text{ km s}^{-1}$, $b = 20 \text{ km s}^{-1}$, $\log N_{\text{SII}} = 13.9 \pm 0.1$). These low-ion velocity components are consistent with the two H I emission components (Wakker et al. 2003; Kalberla et al. 2005) and absorption seen in other low-ionization species in COS data (Yao et al. 2011). The strong Si II $\lambda 1260.42$ line, while redward of the Ly α forest region in Mrk 421, can be fitted with two components ($v = -21 \pm 3 \text{ km s}^{-1}$, $b = 28 \pm 3 \text{ km s}^{-1}$, $\log N_{\text{SiII}} = 15.2 \pm 0.1$) and ($v = -117 \pm 5 \text{ km s}^{-1}$, $b = 14 \pm 5 \text{ km s}^{-1}$, $\log N_{\text{SiII}} = 13.1 \pm 0.1$). The last identified Galactic absorber is the weak, blended Mg II $\lambda\lambda 1239.93, 1240.40$ doublet. Assuming a 2:1 ratio of equivalent widths and similar velocity centroids and b -values to the other Galactic lines, we model the system with $v = -21 \text{ km s}^{-1}$, $b = 59 \text{ km s}^{-1}$, and $\log N_{\text{MgII}} = 15.3$.

The sight line toward Mrk 421 is relatively short ($\Delta z = 0.030$), and there is only a single previously-reported (Shull, Stocke, & Penton 1996) intervening Ly α forest system ($z = 0.01014$, $\lambda = 1228.0 \text{ \AA}$). This moderate-strength Ly α line is well-fitted by a Voigt profile with parameters ($z = 0.01013$, $b = 19 \pm 1 \text{ km s}^{-1}$, $W_\lambda = 76 \pm 4 \text{ m\AA}$, $\log N_{\text{HI}} = 13.25 \pm 0.02$) convolved with the COS line spread function (Ghavamian et al. 2009; Kriss 2011). No corresponding metal absorption (e.g., C IV, Si III, etc.) is seen at this redshift.

A weak absorption feature ($W_\lambda = 25 \pm 4 \text{ m\AA}$) is seen at 1246.4 \AA in the coadded spectrum. There are no species commonly seen in the ISM with absorption lines near 1246 \AA , and the normalized spectrum in the 1243 – 1250 \AA range is free of line-removal artifacts. The most likely identification of this feature is a weak Ly α forest system with fit parameters $cz = 7582 \pm 8 \text{ km s}^{-1}$ ($z = 0.0253$), $b = 52 \pm 12 \text{ km s}^{-1}$, and $\log N_{\text{HI}} = 12.7 \pm 0.1$.

The spectrum is divided by the model (offset curve in the top panel of Figure 1) to give a normalized spectrum, with all identified absorption and emission features removed (Figure 1, lower panel). With the exception of a few narrow line-removal artifacts, the normalized spectrum shows a remarkably uniform appearance over the range $1218 \text{ \AA} \lesssim \lambda \lesssim 1257 \text{ \AA}$.

3. WHIM ABSORPTION TOWARD MRK 421

Given a few input parameters, we can model the expected appearance of a BLA. These parameters can be

TABLE 1
MRK 421 WHIM ABSORBER PARAMETERS

Quantity	$z = 0.011$	$z = 0.027$	Units	Source ^a
UV/X-ray Measurements				
cz	3300 ± 300	8090 ± 300	km s^{-1}	N05
$N_{\text{O VII}}$	1.0 ± 0.3	0.7 ± 0.3	10^{15} cm^{-2}	N05
$N_{\text{O VI}}$	< 1.5	< 1.5	10^{13} cm^{-2}	S05
$N_{\text{N VII}}$	0.8 ± 0.4	1.4 ± 0.5	10^{15} cm^{-2}	N05
$\log T$	6.13 ± 0.39^b	6.15 ± 0.15^c	K	N05
Implied Ly α Absorber Parameters				
b_{therm}	148^{+84}_{-53}	152^{+28}_{-24}	km s^{-1}	
$\log N_{\text{HI}}^d$	$12.5^{+0.6}_{-0.2}$	12.7 ± 0.2	$Z_{0.1}^{-1} \text{ cm}^{-2}$	
$W_{\text{Ly}\alpha}^d$	18^{+55}_{-8}	26^{+11}_{-8}	$Z_{0.1}^{-1} \text{ m\AA}$	
τ_0	0.016	0.025		
SL	1.9	2.7	σ	

^a N05 = Nicastro et al. 2005a (*Chandra*); S05 = Savage et al. 2005 (*FUSE*)

^b Inferred from O VI/VII/VIII ratios

^c Inferred from N VI/VII ratios

^d Assuming $Z = 0.1 Z_{\odot}$. See text for details.

assumed for WHIM absorbers in general, or they can be derived from X-ray WHIM measurements and a few basic assumptions. For general single-phase WHIM gas with total hydrogen column density N_H at temperature T , the neutral hydrogen column density is $N_{\text{HI}} = f_{\text{HI}}(T) N_H$ and the thermal line width is

$$b(T) = (40.6 \text{ km s}^{-1}) T_5^{1/2}, \quad (1)$$

where T_5 is temperature in units of 10^5 K. The neutral fraction as a function of temperature, $f_{\text{HI}}(T)$, can be determined either in collisional ionization equilibrium (CIE) or with a more sophisticated sets of assumptions. In the following analysis, we assume $Z = 0.1 Z_{\odot}$ gas cooling isobarically as tabulated in Gnat & Sternberg (2007). At WHIM temperatures, the hydrogen neutral fraction is identical to that in CIE and the high-ion fractions differ only slightly from their CIE values.

If we start from the reported WHIM parameters derived from the *Chandra* observations, we can derive the N_{HI} via the additional relationship,

$$N_{\text{HI}} = \frac{f_{\text{HI}}(T)}{f_{\text{O VII}}(T)} \frac{N_{\text{O VII}}}{(O/H)_{\odot} Z}. \quad (2)$$

Taking the reported Nicastro et al. X-ray detections at face value, the $cz = 3300 \text{ km s}^{-1}$ X-ray absorber is assumed to have T ranging from 5.5×10^5 K to 3.3×10^6 K, based on O VI/O VII/O VIII column density detections and limits. The $cz = 8090 \text{ km s}^{-1}$ system is inferred to have a somewhat narrower temperature range, $T = 1 - 2 \times 10^6$ K, from N VI/N VII ratios and an O VI non-detection (Savage et al. 2005). These WHIM parameters predict Ly α absorbers with column density $\log N_{\text{HI}} = 12.4 - 13.3$, $b = 95 - 233 \text{ km s}^{-1}$, and $W_{\lambda} = 13 - 100 \text{ m\AA}$ at the $z = 0.011$ absorber; and $\log N_{\text{HI}} \approx 12.7$, $b = 130 - 180 \text{ km s}^{-1}$, and $W_{\lambda} = 10 - 34 \text{ m\AA}$ at $z = 0.027$ (Table 1). We assume $(O/H)_{\odot} = 4.90 \times 10^{-4}$ (Asplund et al. 2009) and $Z = 0.1 Z_{\odot}$. Lower abundances of oxygen would scale these predictions upwards.

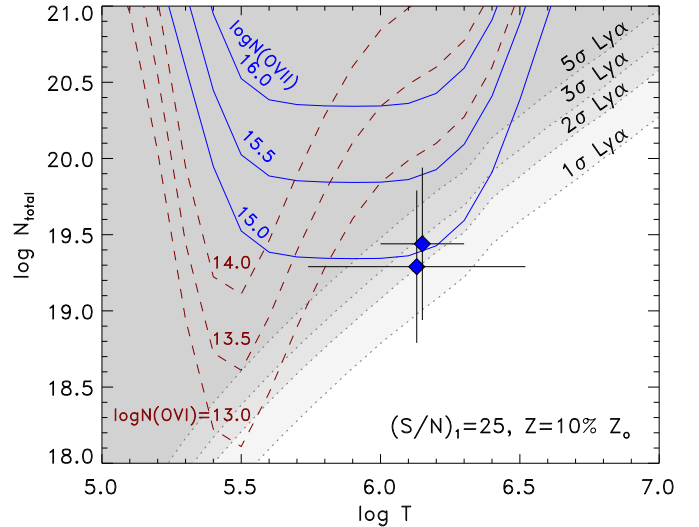


FIG. 2.— The detection limits for WHIM gas via broad Ly α absorption depend on the parameters of the absorber and the quality of the far-UV spectrum. In HST/COS data with $(S/N)_1 \approx 25$ per pixel, idealized, unblended BLAs can be detected at $1 - 5 \sigma$ significance levels as shown by the dotted contours. Typical detection limits for several different column densities of O VII (blue, solid) and O VI (red, dashed) are shown for an assumed metallicity of $Z = 0.1 Z_{\odot}$. Metal line diagnostics scale as Z^{-1} on the vertical axis. Blue diamonds show the parameter-space location of the two Nicastro et al. (2005a) claimed WHIM detections with their uncertainties.

3.1. Signal-to-Noise and Significance Levels

The predicted BLAs are very weak (line-center optical depth $\tau_0 < 3\%$) and much broader than the $\sim 18 \text{ km s}^{-1}$ instrumental resolution of COS. They will be difficult to detect in even high-quality HST/COS spectra and will require a good understanding of the signal-to-noise ratio and systematics in the data. The per-pixel scatter in the normalized, coadded data gives signal-to-noise per pixel $(S/N)_1 \equiv \sigma^{-1} = 25 \pm 1$ over the Ly α forest wavelength range. In the Poissonian ideal, pixel-to-pixel noise is uncorrelated, and combining adjacent pixels results in lower noise (and hence higher S/N) by the square root of the number of pixels binned. We find that binning or smoothing the line-less, normalized data by x pixels results in an empirical relationship $(S/N)_x = (S/N)_1 x^{0.38 \pm 0.02}$, consistent with the behavior in other datasets over a wider wavelength range (Keeney et al. 2011). The fact that the index on x is less than 0.5 shows that the noise in adjacent pixels is correlated to some degree, i.e., fixed pattern noise exists in the data.

The significance level of a detection depends on the observed equivalent width W_{λ} and the S/N of the data. Following the method of Keeney et al. (2011) (their equation A6), we calculate the significance level, SL , of an absorption feature in data binned by x pixels as

$$SL(x) = \frac{f_c(x) W_{\lambda} (S/N)_x}{\Delta \lambda_x} = \frac{f_c(x) W_{\lambda} (S/N)_1 x^{0.38}}{x \Delta \lambda_0}, \quad (3)$$

where $f_c(x)$ is the fraction of the total line profile encompassed by x pixels. For lines much broader than the instrumental resolution, Keeney et al. find that $SL(x)$ is maximized when the data are binned to approximately

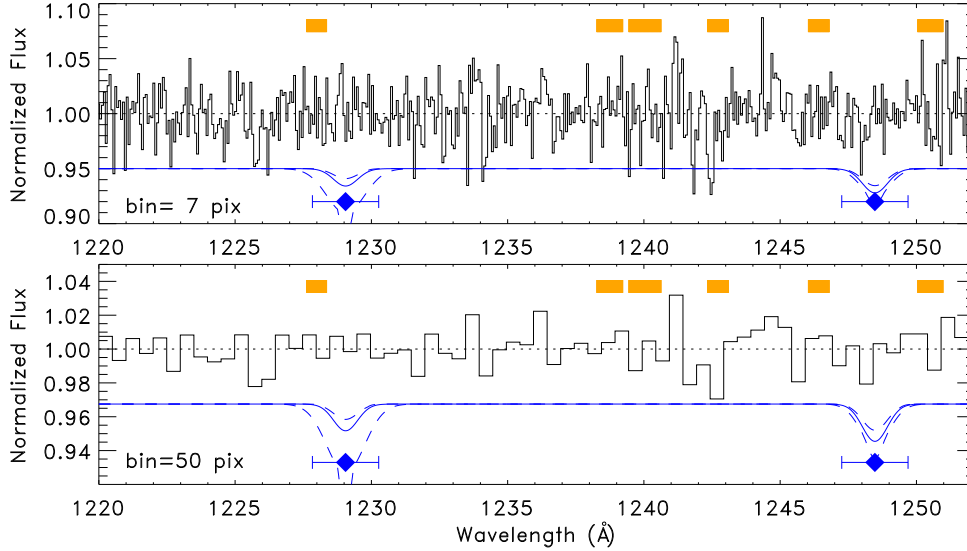


FIG. 3.— Predicted broad Ly α absorbers superimposed on the normalized, line-less COS spectrum of Mrk 421. In the top panel, the COS data are binned to seven pixels (~ 1 resolution element, ~ 17 km s $^{-1}$). Orange bars show regions where narrow absorption features have been modeled out of the spectrum. The blue curves offset below the data show the range of BLA absorption profiles predicted from the O VII detections (solid blue lines) and $\pm 1\sigma$ uncertainties in T and $N(\text{O VII})$ (dashed blue lines) of Nicastro et al. (2005a) as listed in Table 1. Blue diamonds and horizontal error bars show the velocity centroids and ± 300 km s $^{-1}$ uncertainty of the *Chandra* detections. The bottom panel shows the improvement in $(S/N)_x$ obtained by binning the data by 50 pixels. Optimal binning for BLAs at $T \sim 10^6$ K is ~ 100 pixels.

the FWHM of the line or $x \approx 2\sqrt{\ln 2}b$ and that this binning encompasses $f_c(x) = 76\%$ of the total line area. Since each COS pixel in the region of the Ly α forest is approximately 2.4 km s $^{-1}$, this means

$$SL(b) = 0.095 \times W_\lambda \frac{(S/N)_1}{b^{0.62}}, \quad (4)$$

with W_λ in units of mÅ and b in km s $^{-1}$.

Applying Eq. 4 to observed lines, we confirm that the Ly α forest line at 1228.0 Å is highly significant ($SL \sim 30\sigma$). The weak absorption feature at 1246.4 Å assumed to be Ly α at $z = 0.0253$ is a $\sim 5\sigma$ detection in optimally-binned data. Similarly, the stronger (1238.82 Å) line of the Galactic N V doublet is a $\sim 9\sigma$ detection and the blended Galactic Mg II doublet is significant at $\sim 3\sigma$.

3.2. WHIM Parameter Space Accessible by BLA

Figure 2 shows the temperature and total column density parameter space in which we might expect WHIM systems. HST/COS data with $(S/N)_1 = 25$ are sensitive to BLAs in the upper left half of the parameter space. Also shown are the regions in which WHIM could be detected via X-ray (O VII) and UV (O VI) metal-line diagnostics at various column densities in $Z = 0.1 Z_\odot$. The metal-line sensitivity limits scale on the vertical axis as Z^{-1} gas.

Can we confirm or disprove the X-ray WHIM detections based on the COS data? Figure 3 shows the COS data with identified absorption features removed (see Fig. 1) and then binned to 7 and 50 pixels in the upper and lower panels, respectively. The WHIM absorbers predicted from the X-ray measurements would appear at $\lambda \sim 1230$ Å and $\lambda \sim 1249$ Å (blue diamonds), both with a velocity uncertainty of ± 300 km s $^{-1}$ from N05. As predicted, broad features appear more significant in the lower panel where the pixel-to-pixel noise has been

reduced and the binning width is closer to the characteristic line width. The N05 WHIM absorbers modeled via Eq. 3 are predicted to produce BLAs with doppler widths $b \approx 150$ km s $^{-1}$ and equivalent widths of ~ 18 and ~ 26 mÅ for the $z = 0.011$ and $z = 0.028$ features, respectively (blue curve in Figure 3). From Eq. 4, these would be significant (modulo the considerable range in predicted BLA properties; see Table 1) at the 1.9σ and 2.7σ levels in $(S/N)_1 = 25$ HST/COS data binned to ~ 100 pixels.

It is clear from Figure 3 that no $\sim 2 - 3\sigma$ absorption features appear in the COS data consistent in either line profile or centroid with the predicted WHIM absorbers. The claimed Great Wall WHIM detection should appear at $2 - 3\sigma$ significance at 1248.5 ± 1.2 Å, but is not seen in the COS data. The 1246.4 Å feature was discussed above and was removed from the residual spectrum in Figure 3. While relatively broad for a Ly α feature ($b = 52 \pm 12$ km s $^{-1}$; $T \lesssim 10^5$ K), it is inconsistent with the Nicastro et al. O VII detection at $cz = 8090 \pm 300$ km s $^{-1}$ in both redshift and inferred temperature. The 1228.0 Å Ly α line is consistent in redshift with the claimed $z = 0.011$ O VII system, but is far too narrow to arise in gas at $T \sim 10^6$ K.

We therefore rule out WHIM absorption for the two systems with the redshift, temperature and metallicity reported by Nicastro et al. (2005a) at a $\gtrsim 2\sigma$ level. However, if lower O VII column densities, higher temperatures, or higher metallicities are assumed, the (N_H, T) parameter space locations of the claimed WHIM systems move toward the lower right in Figure 2 and would not be detectable in the current COS data.

Two additional weak features become apparent in Figure 3 in locations unrelated to the O VII-predicted BLAs. While both appear significant in the highly-binned lower panel of Figure 3, they are best fitted as single, narrow

components more typical of the photoionized Ly α forest. The first is a feature near 1225.8 Å, a region uncontaminated by narrow absorption lines. It is well-fitted as a $\sim 4\sigma$ narrow Ly α system ($b = 25 \pm 11 \text{ km s}^{-1}$, $W_\lambda = 13 \pm 4 \text{ mÅ}$, $\log N_{\text{HI}} = 12.4 \pm 0.1$) at $z = 0.0083$. The second residual feature appears as an absorption excess in the weaker Galactic N V line at 1242.5 Å. Measurement of this feature is complicated by the overlying N V absorption, but if the absorption profile of the stronger N V line is applied to the weaker line, the residual can be fitted as a $\sim 5\sigma$ feature: $b \sim 27 \text{ km s}^{-1}$, $W_\lambda \sim 19 \text{ mÅ}$, $\log N_{\text{HI}} \sim 12.6$, $z = 0.0220$ if interpreted as Ly α .

4. CONCLUSIONS AND IMPLICATIONS

The Nicastro et al. (2005a) claims of O VII absorbers toward Mrk421 were met with a great deal of skepticism in the X-ray community (Kaastra et al. 2006; Rasmussen et al. 2007). Even the more significant $z = 0.027$ O VII system in the Great Wall ($N_{\text{OVII}} \approx 7 \times 10^{14} \text{ cm}^{-2}$) is only a $\sim 2 \text{ mÅ}$ feature in the *Chandra* LETG data and relies critically on the continuum model in the 21 – 23 Å region. While Mrk421 has been observed for a total of > 200 ksec over many different observing campaigns and features some of the highest S/N data for any extragalactic X-ray target, a more reliable O VII detection limit may require $N_{\text{OVII}} \gtrsim 3 \times 10^{15} \text{ cm}^{-2}$ ($\gtrsim 5 \text{ mÅ}$). Note that the strong ($N_{\text{OVII}} \sim 10^{16} \text{ cm}^{-2}$) O VII absorption at $z = 0$ toward Mrk421 is uncontroversial. Indeed, it is typical of $z = 0$ absorption seen in numerous extragalactic sight lines (Fang et al. 2002; Fang, Sembach, & Canizares 2003; McKernan, Yaqoob, & Reynolds 2004; Nicastro et al. 2002, 2005a; Wang et al. 2005; Williams et al. 2006; Buote et al. 2009) and is thought to arise in hot gas in the Galactic halo.

In this paper we highlight the diagnostic power of thermally-broadened Ly α absorbers in far-UV spectra as tracers of WHIM gas. Mrk421 was observed for less than half an hour (1.7 ksec or half an *HST* orbit) in the blue G130M mode of the Cosmic Origins Spectrograph, and yet it reaches WHIM detection levels comparable to those in > 200 ksec of X-ray observations with *Chandra*. Based on these high-quality data, we can rule out the existence of WHIM gas over a large region of (T, N_H) parameter space (see Figures 2, 3) along much of the Mrk421 sight line. Specifically, we rule out the existence of broad Ly α counterpart absorption to the claimed O VII WHIM absorbers at $z = 0.011$ and $z = 0.027$ (Nicastro et al. 2005a,b) at $\sim 2\sigma$ level. We cannot, however, rule out the existence of the claimed WHIM absorbers if their metallicities are higher than the assumed $Z > 0.1 Z_\odot$, if the O VII column densities are at the lower limits of their reported ranges, or if the temperatures are higher than the $\sim 1 - 2 \times 10^6 \text{ K}$ inferred from ion ratios (Nicastro et al. 2005a,b; Savage et al. 2005). The Ly α absorption in any of these systems would then be below the detection limit of the current COS data.

The search for missing baryons has long centered on

the gas in the WHIM phase via one of several techniques. Roughly one hundred low- z O VI detections have been reported in ~ 30 sight-lines (Danforth & Shull 2008; Tripp et al. 2008; Thom & Chen 2008) which give a statistically-significant sample of lower temperature, higher metallicity WHIM baryons ($T < 10^6 \text{ K}$; $Z > 0.1 Z_\odot$; see red contours in Figure 2). However, while the presence of these absorbers is agreed upon in most cases, their interpretation as WHIM gas is still controversial in roughly half the cases (see, Danforth 2009). X-ray metal lines such as O VII seem to present a more secure identification of WHIM absorption, but suffer from small-number statistics and are still at or beyond the cutting edge of current X-ray instruments. Different, complementary techniques must be employed to verify the phase membership of the O VI systems and confirm the presence of X-ray WHIM absorbers.

The most convincing X-ray WHIM detections have relied on targeted searches of nearby supercluster filaments like the Sculptor Wall detection (Buote et al. 2009; Fang et al. 2010), the Pisces-Cetus Supercluster, and the Far Sculptor Wall (Zappacosta et al. 2010). The Sculptor Wall (at $z = 0.030 \pm 0.002$ in the direction of the blazar target H 2356–309) used both *Chandra* ACIS and *XMM-Newton* RGS to detect the O VII K α absorption line at $z = 0.032$. The O VIII detection at $z = 0.055$ (Fang et al. 2002) towards PKS 2155–304 is coincident with a group of narrow Ly α lines at the redshift of a group of spiral galaxies (Shull et al. 1998; Shull, Tumlinson, & Giroux 2003). In many ways, the search for WHIM along the Mrk421 sight line (whether via X-ray or UV metal ions or BLAs) should also be considered a targeted search, since this object lies just behind a section of the Great Wall, whether or not WHIM gas is ultimately confirmed.

Although the current dataset appears to rule out the WHIM detections claimed by N05, due to the importance of these claims, we plan to re-observe Mrk421 with COS in *HST* Cycle 19. Deeper observations will either reveal a BLA feature below the current detection limit or place stronger constraints on WHIM gas in the sight line. Either way, the detection/non-detection of WHIM in the Great Wall will add an important data-point to the correlation of hot baryons and large-scale structure. The covering factor of WHIM gas around galaxy filamentary structure has significant impact on our understanding of the missing baryon problem at low- z . Correlating the much larger catalogs of low- z O VI detections (Danforth & Shull 2008; Tripp et al. 2008; Thom & Chen 2008) with galaxy redshift surveys may reveal additional filament-WHIM correspondence, and document the WHIM non-detections in similar LSS features.

This work was supported by NASA grants NNX08AC146 and NAS5-98043 to the University of Colorado at Boulder. CWD acknowledges feedback from F. Nicastro and M. Elvis.

Facilities: HST(COS)

REFERENCES

- Asplund, M., Grevesse, N., Sauval, A. J., & Scott, P. 2009, *ARA&A*, 47, 481
- Buote, D. A., Zappacosta, L., Fang, T., Humphrey, P. J., Gastaldello, F. & Tagliaferri, G. 2009, *ApJ*, 695, 1351

- Cen, R., & Ostriker, J. P. 1999, *ApJ*, 519, L109
- Danforth, C. W., & Shull, J. M. 2005, *ApJ*, 624, 555
- Danforth, C. W., & Shull, J. M. 2008, *ApJ*, 279, 194 (DS08)
- Danforth, C. W. 2009, *AIP Conf. Proc.* 1135, 8, eds. G. Sonneborn, M. E. van Steenberg, H. W. Moos, & W. P. Blair (arXiv:0812.0602)
- Danforth, C. W., Stocke, J. T., & Shull, J. M., 2010a, *ApJ*, 710, 613
- Danforth, C. W., Keeney, B. A., Stocke, J. T., Shull, J. M., & Yao, Y. 2010b, *ApJ*, 720, 976
- Davé, R., et al. 1999, *ApJ*, 511, 521
- Davé, R., et al. 2001, *ApJ*, 552, 473
- Fang, T., Marshall, H. L., Lee, J. C., Davis, D. S., & Canizares, C. R., 2002, *ApJ*, 572, L127
- Fang, T., Sembach, K. R. & Canizares, C. R. 2003, *ApJ*, 586, L49
- Fang, T., Buote, D. A., Humphrey, P. J., Canizares, C. R., Zappacosta, L., Maiolino, R., Tagliaferri, G. & Gastaldello, F. 2010, *ApJ*, 714, 1715
- Ghavamian, P., et al. 2009, COS Instrument Science Report 2009-01(v1), Preliminary Characterization of the Post-Launch Line Spread Function of COS (Baltimore: STScI)
- Gnat, O. & Sternberg, A. 2007, *ApJS*, 168, 213
- Green, J. C. et al. 2011, *ApJ*, submitted
- Kaastra, J., Werner, N., den Herder, J. W., Paerels, F., de Plaa, J., Rasmussen, A. P., & de Vries, C. 2006, *ApJ*, 652, 189
- Kalberla, P. M. W., Burton, W. B., Hartmann, D., Arnal, E. M., Bajaja, E., Morras, R., & Poppel, W. G. L., 2005, *A&A*, 440, 775
- Keeney, B. A., et al. 2011, in prep.
- Kriss, G. A. 2011, COS Instrument Science Report 2011-01(v1), Improved Medium Resolution Line Spread Functions for COS FUV Spectra (Baltimore: STScI)
- de Lapparent, V., Geller, M. J. & Huchra, J. P. 1986, *ApJ*, 302, L1
- Lehner, N., Savage, B. D., Richter, P., Sembach, K. R., Tripp, T. M., & Wakker, B. P. 2007, *ApJ*, 658, 680
- McKernan, B., Yaqoob, T., & Reynolds, C. S. 2004, *ApJ*, 617, 232
- Nicastro, F., Zezas, A., Drake, J., Elvis, M., Fiore, F., Fruscione, A., Marengo, M., Mathur, S., & Bianchi, S. 2002, *ApJ*, 573, 157
- Nicastro, F., Mathur, S., Elvis, M., Drake, J., Fiore, F., Fang, T., Fruscione, A., Krongold, Y., Marshall, H., & Williams, R. 2005a, *ApJ*, 629, 700
- Nicastro, F., Mathur, S., Elvis, M., Drake, J., Fang, T., Fruscione, A., Krongold, Y., Marshall, H., Williams, R., & Zezas, A., 2005b, *Nature*, 433, 495
- Oppenheimer, B. D., & Davé, R. A. 2008, *MNRAS*, 395, 1875
- Oppenheimer, B. D., Davé, R., Katz, N., Kollmeier, J. A., & Weinberg, D. H., 2011, *MNRAS*, submitted (arXiv:1106.1444)
- Penton, S. V., Stocke, J. T., & Shull, J. M. 2000, *ApJS*, 130, 121
- Osterman, S., et al. 2011, *Ap&SS*, in press
- Rasmussen, A. P., Kahn, S. M., Paerels, F., den Herder, J. W., Kaastra, J., & de Vries, C. 2007, *ApJ*, 656, 129
- Richter, P., Savage, B. D., Tripp, T. M., & Sembach, K. R. 2004, *ApJS*, 153, 165
- Richter, P., Savage, B. D., Sembach, K. R., & Tripp, T. M. 2006, *A&A*, 445, 827
- Savage, B. D., Wakker, B. P., Fox, A. J., & Sembach, K. R. 2005, *ApJ*, 619, 863
- Sembach, K. R., Tripp, T. M., Savage, B. D. & Richter, P., 2004, *ApJS*, 155, 351
- Shull, J. M., Stocke, J. T., & Penton, S. 1996, *AJ*, 111, 72
- Shull, J. M., et al. 1998, *AJ*, 116, 2094
- Shull, J. M., Tumlinson, J., & Giroux, M. 2003, *ApJ*, 594, L107
- Smith, B. D., Hallman, E. J., Shull, J. M. & O'Shea, B. W. 2011, *ApJ*, 731: 6
- Stocke, J. T., Danforth, C. W., & Perlman, E. S. 2011, *ApJ*, 732, 113
- Thom, C., & Chen, H.-W. 2008, *ApJ*, 683, 22
- Tripp, T. M., Sembach, K. R., Bowen, D. V., Savage, B. D., Jenkins, E. B., Lehner, N., & Richter, P. 2008, *ApJS*, 177, 39
- Wakker, B. P., et al. 2003, *ApJS*, 146, 1
- Wang, Q. D., Yao, Y., Tripp, T. M., Fang, T.-T., Cui, W., Nicastro, F., Mathur, S., Williams, R. J., Song, L., Croft, R. 2005, *ApJ*, 635, 386
- Williams, R. J., Mathur, S., Nicastro, F., & Elvis, M. 2006, *ApJ*, 642, L95
- Williams, R. J., Mulchaey, J. S., Kollmeier, J. A., & Cox, T. J. 2010, *ApJ*, 724, L25
- Yao, Y., Shull, J. M., & Danforth, C. W. 2011, *ApJ*, 728, L16
- Zappacosta, L., Nicastro, F., Maiolino, R., Tagliaferri, G., Buote, D. A., Fang, T., Humphrey, P. J., & Gastaldello, F. 2010, *ApJ*, 717, 74